Proceedings of the 3rd Annual
IEEE Conference on Automation Science and Engineering
Scottsdale, AZ, USA, Sept 22-25, 2007

Multi-Probe Micro-Assembly

John Wason, William Gressick, John T. Wen

Center for Automation Technologies & Systems
Rensselaer Polytechnic Institute
Troy, NY 12180
{wasonj,gressw2,wenj}@rpi.edu

Jason Gorman, Nick Dagalakis

Intelligent Systems Division
National Institute Of Standards and Technology
Gaithersburg, Maryland 20899-8230
{gorman,nicholas.dagalakis}@nist.gov

***Abstract*— This paper describes the algorithm development and experimental results of a multi-probe micro-assembly system. The experimental testbed consists of two actuated probes, an actuated die stage, and vision feedback. The kinematics relationships for the probes, die stage, and part manipulation are derived and used for calibration and kinematics-based planning and control. Particular attention has been focused on the effect of adhesion forces in probe-part and part-stage contacts in order to achieve grasp stability and robust part manipulation. By combining pre-planned manipulation sequences and vision based manipulation, repeatable spatial (in contrast to planar) manipulation and insertion of a sub-millimeter part has been demonstrated. The insertion process only requires the operator to identify two features to initialize the calibration, and the remaining tasks involving part pick-up, manipulation, and insertion are all performed autonomously.**

I. Introduction

Modern silicon fabrication technologies have provided the ability to create electro-mechanical devices on a micro-scale using techniques originally designed for the fabrication of integrated circuits. While the understanding of the behavior of these devices has advanced significantly, a reliable method for assembling parts still does not exist [1]. Currently most devices are designed to be monolithic, and do not require assembly. This approach has made significant advances, but the resulting monolithic devices are severely limited in functionality when compared to spatial devices that have been assembled from multiple parts. This research investigates the possibility of spatial micro-assembly using multiple sharp probes instead of using grippers or other exotic methods. The initial problem posed was to simply insert a small (sub-millimeter) part into a slot. The part needs to be lifted, rotated out of plane, and inserted. Figure 1 shows a photo of the part before it is picked up and after it has been inserted. This simple task is intended to be a first step toward assembling complex spatial structures involving multiple parts.

The Intelligent Systems Division (ISD) at NIST has developed MEMS nanopositioners and micro-assembly techniques for micro and nano technology. Work on MEMS devices has focused on the development of two degree of freedom and three degree of freedom parallel nanopositioning devices that are several hundred microns in size [2], [3]. Micro-assembly work has focused on the the use of probes to manipulate small spheres with force and vision feedback [4], [5]. The long term goal of the current project is to combine these two technologies to produce a MEMS spatial six degree of freedom nanopositioner through the use of planar positioners and spatial micro-assembly.

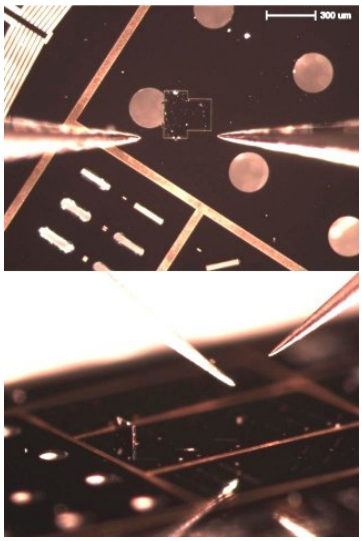

Fig. 1. NIST Part Before and After Insertion

Assembly of a complex spatial mechanism requires a micro-assembly technique that is both flexible and robust. Because of the complexity of the mechanism and the limited knowledge of the behavior of MEMS devices, it is likely that several design iterations will be needed to produce a working device. The assembly process will need to be adaptable to numerous different designs. A flexible micro-assembly process will also allow the MEMS device to be customized to different applications without the need to redesign the assembly process. Current micro-assembly techniques do not meet the requirements for flexibility and robustness. This research uses multiple sharp-tip (2 μm diameter) probes to produce an assembly process that satisfies these requirements. The following sections describe the insertion task, the hardware and kinematics of the system developed for this task, the

This work is supported in part by the National Institute of Stands and Technology (NIST) under the Small Grant program and the Center for Automation Technologies and Systems (CATS) under a block grant from the New York State Office of Science, Technology, and Academic Research (NYSTAR).

John Wen is supported in part by the Outstanding Overseas Chinese Scholars Fund of Chinese Academy of Sciences (No. 2005-1-11).

kinematics of the part once both probes have contacted, the expected contact force, and the effect of adhesion forces on the assembly process.

II. Micro-Insertion Task

The single part micro-insertion task considered in this research is intended to be an iterative step toward multiple part micro-assembly. A part measuring 300 microns square is shaped to fit vertically into a slot (Figure 1). The micro-assembly system needs to grab and lift the part off the surface and then rotate it out of plane to the vertical position. Once rotated, the part is aligned with a slot and inserted. An automated insertion process has been developed utilizing vision feedback. The operator locates the part and clicks on two points on the part to center and pre-align it. The rest of the process is automatic. The manipulation has shown to be very robust. With the current system an entire insertion process takes around 5 minutes, but this can be reduced by the use of faster cameras and image processing software. The steps of the insertion process and the current method used for each step is listed below.

1. Initialize and Calibrate System
   a. Due to tight assembly tolerances, the system must be calibrated every startup. Vision is used to determine alignment between different components.
2. Locate Part
   a. The Part is initially placed randomly on die and must be located with a point-and-click operator assisted operation.
3. Move close and grab part
   a. The die stage is manipulated so the part is within the manipulator workspace.
   b. The probes are lowered to the correct height using vision feedback. The distance between the reflection of the part is used to determine the height.
   c. The left probe is moved to a small distance away from the desired contact point, and then slowly moved into the part until the part moves slightly.
   d. Right probe is moved to a point close to the part, then moved into the part a pre-determined distance to achieve the correct force.
   e. Thresholding and edge tracing operations are used to locate the part and probes throughout the grasp operation
4. Rotate part to vertical position
   a. A third unactuated probe is used to achieve an out-of-plane rotation. The two actuated probes generate a curved motion about the third probe to rotate the part
   b. The part is rotated 20 to 30 degrees past vertical to assist detection for insertion.
   c. The rotation is based on the execution of a pre-planned autonomous scripted motion (without the use of vision feedback).
5. Insert part
   a. The part is moved close to the insertion slot.

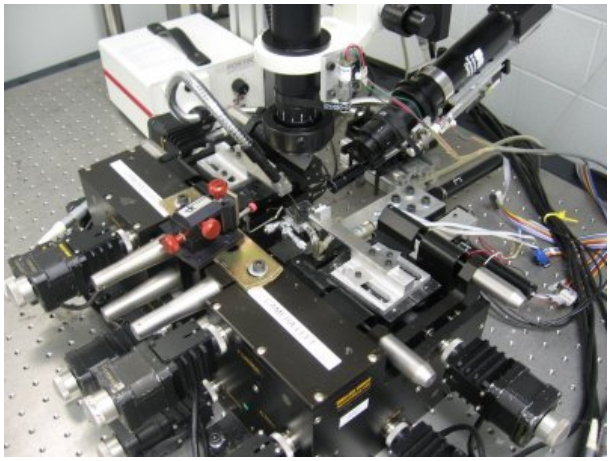

Fig. 2. Photo of Micro Insertion System

   b. The bottom edge of the part and the position of the slot are detected through vision edge tracing.
   c. The part is lowered into the slot, then the part is rotated vertical during insertion.

III. Hardware Overview

The micro-assembly system developed at the Center for Automation Technologies and Systems (CATS) at RPI is a combination of hardware and software configured for telerobotic, operator assisted, and fully automated assembly tasks. Several different components have been integrated to produce an effective system. Figure 2 is a photograph of the manipulation area, and Figure 3 is a photo of the operator station. The major components of the systems are listed below.

- Two 9-degree-of-freedom (DOF) Melles-Griot nano-positioner stages for the probes
- A 3-DOF manual stage for an unactuated third probe
- A 3-DOF actuated die stage
- Two 1.2 Megapixel C-mount microscope Firewire cameras with actuated zoom
- Advanced control electronics based on custom and off-the-shelf components
- MATLAB and Visual Basic based software interface

This system has been configured for assembling various types of micro-systems. Though the system design is initially intended for 3D micro-assembly tasks described here, it has shown to be easily adoptable for other micro-manipulation tasks, such as optical fiber manipulation, alignment, and assembly.

IV. System Kinematics

The basic kinematic design of the system is based on the two probe manipulators operating over a silicon die containing the device being assembled. The two manipulators are sharp-tipped probes designed to manipulate small silicon parts. The probes are mounted on two six degree of freedom ThorLabs (Formerly Melles-Griot) NanoMax 600 positioners

Fig. 3. Photo of Operator Station

in an opposed configuration. These positioners provide extremely high accuracy (10nm) using a combination of stepper and piezo actuators. The die itself is mounted on a 3-DOF stage mounted between the two 6-DOF stages that allows for translation and rotation in the plane of the die. The die may then be moved into and out of the relatively limited work space of the die probes. The following sections describe the kinematics of the different subsystems.

A. Probe Kinematics

The stepper motors provide approximately 1μm translational and 1 micro-degree rotational resolution. The piezo drives provide approximately 10nm translational and 10ndeg rotational resolution. The rotational axes intersect at a common point which is fixed with respect to the prismatic joints. As the positioning stage was originally designed for fiber alignment, this point is located several centimeters away from the rotational point. This means that the position of this point in the moving frame must be determined in order to maintain a specific rotation point in the workspace.

The kinematics for the left probe are derived below. Note that the kinematics for the right probe are identical to the left and simply requires changing the subscript from L to R in all the equations.

$$R_{L_{36}} = R_{L_{T_L 0}} = e^{\hat{h}_{Lz}\theta_{L4}} e^{\hat{h}_{Ly}\theta_{L5}} e^{\hat{h}_{Lx}\theta_{L6}}$$
$$p_{0T_L} = p_{0L_1} + h_{Lx}\theta_{L1} + h_{Ly}\theta_{L2} + h_{Lz}\theta_{L3} + R_{L_{36}} p_{L_6 T_L}.$$

The $\hat{\cdot}$ denotes the cross product operation, h_i is the axis of rotation of joint i in the ith frame, p_{ij} is the vector from point i to j represented in the ith frame, and the numerical subscripts denote the corresponding joints.

The extremely small dimensions of the parts being assembled means that it is impossible to align or measure all the dimensions of the system to a high enough degree of accuracy. Instead, a calibration routine using the cameras is used. The overall kinematics is depicted in Figure 4.

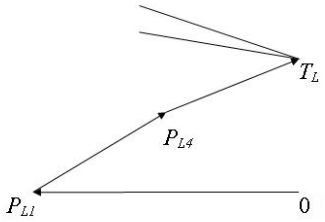

Fig. 4. Probe Kinematics

The probe is perturbed to a hundred different positions, and the unknown dimensions are run through a minimization algorithm. For the positioning stages, it is assumed that the Z axis is aligned with the world z axis. This means that the only unknowns are the rotation of the entire positioning mechanism about the Z axis (parameterized by the scalar ϕ_L), the vector from the origin to the zero translation position of the common rotation point (p_{0L_1}, three parameters), and the vector from the common rotation point after all actuators to the tool tip ($p_{L_6 T_L}$, three parameters). Together, these are the 7 parameters that need to be estimated. All 7 parameters are determined through a single minimization scheme. The joint motion axes are determined by the initial rotation about the z-axis of the entire mechanism, ϕ_L:

$$R_L = e^{\hat{z}\phi_L}\,,\; h_{Lx} = R_L x\,,\; h_{Ly} = R_L y\,,\; h_{Lz} = z.$$

The differential kinematics, which is needed for kinematics-based feedback control, is given by:

$$\begin{aligned}
\dot{x}_L &= J_L \dot{\theta}_L \\
\dot{\theta} &= \begin{bmatrix} \dot{\theta}_{L1} & \dot{\theta}_{L2} & \dot{\theta}_{L3} & \dot{\theta}_{L4} & \dot{\theta}_{L5} & \dot{\theta}_{L6} \end{bmatrix}^T \\
J_L &= \begin{bmatrix} 0 & 0 & 0 & h_{Lz} & & \\ h_{Lx} & h_{Ly} & h_{Lz} & \widehat{h_{Lz}} R_{L_{36}} p_{L_6 T_L} & & \\ & & & R_{L_{45}} h_{Ly} & R_{L_{46}} h_{Lx} & \\ & & & \widehat{h_{Ly}} R_{L_{36}} p_{L_6 T_L} & \widehat{h_{Lx}} R_{L_{36}} p_{L_6 T_L} & \end{bmatrix}
\end{aligned}$$

B. Die Stage Kinematics

The die stage is configured to allow the entire portion of a 10mm×10mm device to be accessed by the relatively small 1mm×1mm working area of the manipulation system. While the positioning stages are capable of moving approximately 3mm in all directions, the camera field of view is only about 1mm. The actuated die also allows the manipulation strategy of only moving the part itself very slightly and moving the die under the part when large motions are necessary (so the limited manipulability of the part is compensated by moving the die underneath). The die stage consists of two prismatic joints followed by a rotational joint. The rotation point is located near the center of the camera view when both prismatic joints are in the zero configuration. The mechanism is assumed to be planar, and thus only 5 parameters ($p_{L_{01}}$, $p_{D_3 T_D}$, ϕ_D) need to be calibrated (see Figure 5. The overall

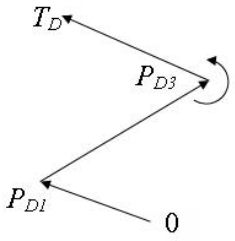

Fig. 5. Die Stage Kinematics

kinematics is described by the equations below:

$$\begin{aligned} R_{D_{23}} &= R_{D_{0T}} = e^{\hat{h}_{Dz}(\theta_{D3}+\theta_{D3(0)})} \\ p_{L_{oT}} &= p_{L_{01}} + h_{Dx}\theta_{D1} + h_{Dy}\theta_{D2} + R_{L_{23}}p_{D_3D_T} \\ R_D &= e^{\hat{z}\phi_D}\,,\; h_{Dx} = R_D x\,,\; h_{Dy} = R_D y\,,\; h_{Dz} = z \\ \dot{x}_D &= J_D\dot{\theta}_D\,,\; \dot{\theta}_D = \begin{bmatrix} \dot{\theta}_{D1} & \dot{\theta}_{D2} & \dot{\theta}_{D3} \end{bmatrix}^T \\ J_D &= \begin{bmatrix} 0 & 0 & h_{Dz} \\ h_{Dx} & h_{Dy} & \widehat{h_{Dz}}R_{D_{23}}p_{D_3T_D} \end{bmatrix}. \end{aligned}$$

C. Part-Probe Closed Loop Kinematics

Manipulation of the NIST part begins with the part lying flat on the surface. To lift the part, the probes are pressed against the edges to create a contact force. The part can then be lifted off the surface and manipulated. During experiments these contacts have behaved as soft-finger contacts, meaning that they do not rotate about the axis normal to the surface of contact. This allows the contact between the probes and the part be represented as a two-axis rotation. This rotation can be treated as two passive joints, allowing for the development of closed-loop differential kinematics based on two probes contacting at the same time. The following equations develop the Jacobian of the extended left probe system to T_p, the tool point of the part (see Figure 6). The vectors p_{LP} and p_{RP} will depend on where the probes make contact and will need to be measured each time the part is lifted.

$$\begin{aligned} R_{LP} &= R_{T_L0}R_{0P}e^{\hat{y}\theta_{LP1}}e^{\hat{z}\theta_{LP2}} \\ \dot{\theta}_{LP} &= \begin{bmatrix} \dot{\theta}_{LP1} & \dot{\theta}_{LP2} \end{bmatrix}^T \\ J'_{LP} &= \begin{bmatrix} R_{0P}(e^{-\hat{z}\theta_{LP2}})y & R_{0P}z \\ R_{0P}(\widehat{e^{-\hat{z}\theta_{LP2}}})yR_{0P}p_{LP} & \widehat{R_{0P}\hat{z}R_{0P}p_{LP}} \end{bmatrix} \\ J_{LP} &= \begin{bmatrix} A_LJ_L & J'_{LP} \end{bmatrix},\; A_L = \begin{bmatrix} I & 0 \\ -(R_{0P}\hat{p}_{LP}) & I \end{bmatrix}. \end{aligned}$$

The same equations hold for the right probe with the subscript L replaced by R.

With the Jacobian determined for both the left and right chains up to T_P, the tool point of the probe, we can write down the task and constraint Jacobians [6]. These Jacobians are then used to determine the differential relationship between the twelve active joints and the part. With this information, it is possible to calculate what joint motions are required to generate a desired motion of the part. Using vision feedback these equations can be used to manipulate

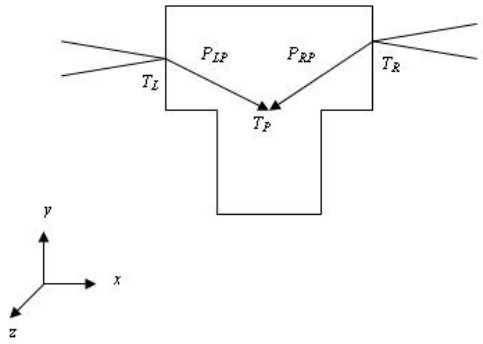

Fig. 6. Part Kinematics

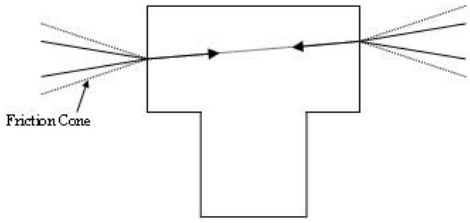

Fig. 7. Probe Friction Cone

and eventually insert the part. The task Jacobian is derived from

$$\begin{aligned} \dot{x}_P &= J_{LP}\begin{bmatrix} \dot{\theta}_L \\ \dot{\theta}_{LP} \end{bmatrix} + J_{RP}\begin{bmatrix} \dot{\theta}_R \\ \dot{\theta}_{RP} \end{bmatrix} \\ &= \underbrace{\begin{bmatrix} A_LJ_L & A_RJ_R \end{bmatrix}}_{J_{Ta}}\underbrace{\begin{bmatrix} \dot{\theta}_L \\ \dot{\theta}_R \end{bmatrix}}_{\dot{\theta}_a} + \underbrace{\begin{bmatrix} J'_{LP} & J'_{RP} \end{bmatrix}}_{J_{Tp}}\underbrace{\begin{bmatrix} \dot{\theta}_{LP} \\ \dot{\theta}_{RP} \end{bmatrix}}_{\dot{\theta}_p}. \end{aligned}$$

The constraint Jacobian is derived from

$$\begin{aligned} J_{LP}\begin{bmatrix} \dot{\theta}_L \\ \dot{\theta}_{LP} \end{bmatrix} - J_{RP}\begin{bmatrix} \dot{\theta}_R \\ \dot{\theta}_{RP} \end{bmatrix} &= 0 \\ \underbrace{\begin{bmatrix} A_LJ_L & -A_RJ_R \end{bmatrix}}_{J_{Ca}}\dot{\theta}_a + \underbrace{\begin{bmatrix} J'_{LP} & -J'_{RP} \end{bmatrix}}_{J_{Cp}}\dot{\theta}_p. \end{aligned}$$

Finally, the active and passive components of the task and constraint Jacobian can be combined into J_P, the part Jacobian. This part Jacobian is useful for the manipulation of the part.

$$\begin{aligned} J_p &= \left(J_{Ta} - J_{Tp}J_{Cp}^{+}J_{Ca}\right) \\ \dot{x}_p &= J_p\begin{bmatrix} \dot{\theta}_L \\ \dot{\theta}_R \end{bmatrix} \\ \begin{bmatrix} \dot{\theta}_L \\ \dot{\theta}_R \end{bmatrix} &= J_p^{+}\dot{x}_p. \end{aligned}$$

V. Grip Stability

The part is gripped by pushing two probes against either side of the part. In practice this has shown to be a very

reliable method to lift the part. Because only two probes are used, it is necessary that the forces be equal and opposite along same line to avoid generating a moment (see Figure 7). The most reliable way to lift the part has been to first align the part using the die stage so that the contact surfaces are perpendicular to the x-axis, and then push the probes against the edge of the part along the x-axis. The part can then be lifted off the die and manipulated spatially.

It has been observed that the part will not rotate about the line between contact points unless it is forced by another feature, creating a soft finger contact. Because of the nature of the friction cones in a soft finger contact and the limited travel of the probe stages, the angular manipulation of the part is limited. The design of the probe mounts and the single axis of measurement a force sensor will eventually supply means that the force can only be applied effectively by translating in the x-axis. This means that the line between the contact point of the left probe and the contact point of the right probe must always be within the friction cone. Assuming a static coefficient of friction of $\mu = .3$,

$$\alpha = atan(.3) = 16^{\circ}.$$

This means that the part can only be manipulated within $\pm 16^{\circ}$ of alignment with the world coordinate frame. This has shown to be a very challenging problem to overcome in micro-insertion. The in-plane rotation can be easily overcome by simply rotating the die stage, but the out-of-plane rotations have shown to be difficult. Two options are to create a fixture that can spin about the contact line a full ninety degrees, or to attempt to spin about this same contact line by producing a moment with a third stationary probe. The latter strategy is adopted and is discussed in Section VII-A.

VI. Probe Deflection

When the probes are pushed against the part, the deflection of the probes is used to maintain contact force (see Figure 8). This compliant joint, with the help of the adhesion forces at the contacts, allows repeatable manipulation within a small angular range. While a force sensor would provide an optimal solution for manipulation, the deflection of the probe is enough to maintain reliable contact with the part. Our experiments have generally shown that 5μm of deflection of the probe in the x-direction is enough to reliably maintain contact without risking damage to the part. The spring constant of the bending of a 1" long Tungsten probe with a 0.51mm diameter is approximately 288.5N/m. This means that at a deflection of 5μm, approximately 1.45mN of force is applied to the part. This is comparable to values encountered by Zesch et al. in force controlled pushing experiments [7].

VII. Adhesion Forces and Orientation Change

At the sub-millimeter scale, the dominant forces affecting manipulation shift from inertia, gravity, and friction to a set of adhesion forces between different objects. In fact, inertia and gravity often become negligible compared to these adhesion forces. Literature on this topic primarily deals with Van Der Waals force, electrostatic attraction, and capillary forces

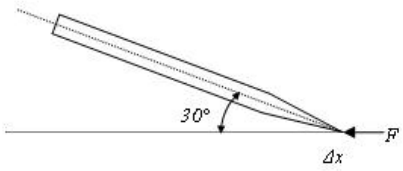

Fig. 8. Probe Deflection

[8]. These forces will cause a part being manipulated to stick to the gripper manipulating it. This has prevented standard micro grippers from behaving the same way that a macro gripper would behave. Instead of the part being released when the gripper is opened, the part simply sticks. Most research in the micro-adhesion area, including Zhou et al., has focused on the Van Der Waals and electrostatic attraction forces [8]. However, these are not the dominant forces for this micro-assembly project. Using the calculations provided in [1], [8] and reasonable parameter assumptions, the Van der Waals attraction force with the 2μm probe contacting silicon is only $1.7 * 10^{-30}$N. At almost any micro-assembly scale this force is negligible. The electrostatic force is considerable stronger, estimated to be between 50 to 100 nN based on the data presented in [8]. This also does not take into account that the probe is grounded, further reducing the possible electrostatic attraction. The force of 100nN is on par with the gravity force of 77nN of the part. The last force is the capillary force, and we hypothesize that this is the dominant force. The part only sticks on the edges where capillary force is strongest, and provides significant adhesion [9]. This behavior is very dependent on the humidity in the room, and environmental changes have caused drastic effects on how this force behaves.

A. Out of Plane Rotation

By using a third probe, it is possible to spin the part about the line between the two actuated probes without the part being dropped. The probes may slide along the long edge of the surface, but the probe tip is held toward the center of the thin edge of the part due to the strong capillary potential that exists at the intersection of the two faces of the part. The use of a third probe for out of plane rotations has shown to be highly successful. A grip force created by deflection in the probes has shown to be adequate for both manipulation and the out of plane rotation. The adhesion forces help prevent the probes from sliding off the edge of the part during this operation.

VIII. Experimental Results

Using the experimental testbed discussed in Section III, we have demonstrated automated manipulation and insertion of a sub-millimeter part through a combination of calibration, vision based motion, and preplanned motion sequences as described in Section II. The process is very repeatable,

although the vision sensing is highly sensitive – features on the die and lighting condition can significantly affect the detection of the part and probes. Figure 9 shows the part at different steps in the procedure. Figure 9(a) shows the part at the beginning of the insertion procedure. Figure 9(b) shows the part after being rotated. Figure 9(c) shows the part after it has been grabbed by the probes using vision feedback. Figures 9(d)-(e) show the part at the start and the end of the out of plane rotation. The part is rotated past 90 deg to assist in sensing the bottom edge of the part with the top camera. Figure 9(f) shows the part and slot after a sequence that pre-aligns the part. Finally, the part is inserted into the slot as shown in Figure 9(g).

IX. Conclusion

This research presents the analysis and experimental results of a probe-based manipulation and insertion in a micro-assembly task. The approach of using multiple sharp-tipped probes and an active die stage, together with pre-planned motion sequences and vision feedback, has shown great promise as a flexible and robust method for 3D micro-manipulation and micro-assembly. Current and future work focuses on the development of repeatable automatic sensing and manipulation of the part and the construction of more complex spatial mechanisms.

References

[1] Q. Zhou, P. Kallio, and H. N. Koivo, "Modeling of micro operations for virtual micromanipulation," in *SPIE Conference on Microrobotics and Microassembly*, vol. 3834, Boston, MA, 1999.

[2] S. Brgna, J. J. Gorman, and N. G. Dagalakis, "Design and modeling of thermally actuated mems nanopositioners," in *SME International Mechanical Engineering Congress and Exposition*, Orlando, FL, 2005.

[3] B. H. Kang, J. T.-Y. Wen, N. G. Dagalakis, and J. J. Gorman, "Analysis and design of parallel mechanisms with flexure joints," *IEEE Transactions on Robotics*, vol. 21, pp. 1179–1185, 2005.

[4] J. J. Gorman and N. G. Dagalakis, "Probe-based micro-scale manipulation and assembly using force feedback," in *International Conference on Robotics and Remote Systems for Hazardous Environments*, Salt Lake City, UT, 2006, pp. 621–628.

[5] D. Haliyo, Y. Rollot, and S. Regnier, "Manipulation of micro-objects using adhesion forces and dynamical effects," in *IEEE International Conference on Robotics and Automation*, Washington, DC, May 2002, pp. 1949 – 1954 vol.2.

[6] J. T.-Y. Wen and L. Wilfinger, "Kinematic manipulability of general constrained rigid multibody systems," *IEEE Transaction on Robotics and Automation*, vol. 15, no. 3, pp. 558–567, June 1999.

[7] W. Zesch and R. S. Fearing, "Alignment of microparts using force controlled pushing," in *SPIE Conference on Microrobotics and Microassembly*, vol. 3834, Boston, MA, 1998, pp. 195–202.

[8] Y. Zhou and B. J. Nelson, "Adhesion force modeling and measurement for micromanipulation," in *SPIE Conference on Microrobotics and Microassembly*, vol. 3519, Boston, MA, 1998, pp. 169–180.

[9] P. Lambert, P. Letier, and A. Delchambre, "Capillary and surface tension forces in the manipulation of small parts," in *Proceedings of the IEEE International Symposium on Assembly and Task Planning*, Besancon, France, July 2003, pp. 54–59.

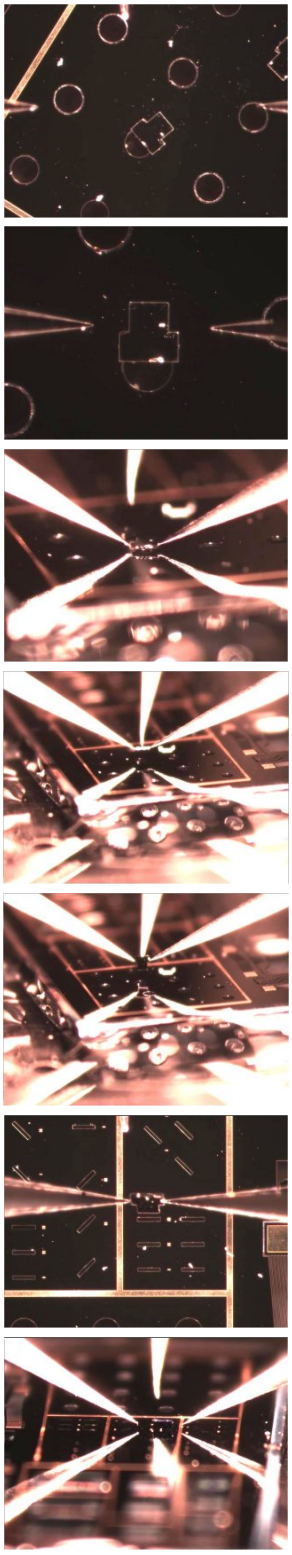

Fig. 9. (a) Initial Part Position (b) Part rotated and probes moved close to part (c) Probes gripping part after automated sequence (d) Part at start of out of plane rotation (e) Part after out of plane rotation (f) Part and slot pre-aligned (g) Part inserted